Journal of Applied Mechanics and Technical Physics, Vol. 43, No. 1, pp. 114–119, 2002

HEAT-AND MASS-TRANSFER CHARACTERISTICS IN A SPATIAL SUBSONIC FLOW AROUND A BLUNT BODY

V. I. Zinchenko, K. N. Efimov,
A. G. Kataev, and A. S. Yakimov

UDC 533.526 + 536.24

A study was performed of methods for controlling thermal regimes in a spatial supersonic flow around a blunt body with the simultaneous use of gas injection from the surface of the porous bluntness and heat flow in the shell material. The effect of the nonisothermicity of the shell wall on the heat- and mass-transfer characteristics in the boundary layer was taken into account by solution of the problem in a conjugate formulation. It is shown that heat conducting materials can be used to advantage to reduce the maximum temperatures in the screen zone.

In the design of high-speed flight vehicles, one of the most complicated problems is the thermal protection of structures. More and more stringent requirements on the accuracy in determining the heat- and mass-transfer characteristics of the shell of a streamline body has led to the necessity of solving the problem in a conjugate formulation [1–3].

With increase in thermal loads, structural materials frequently operate at the limit of their possibilities. Therefore, it is of interest to study highly heat-conducting materials, which ensure a decrease in surface temperature T_w. An alternative solution of the problem is apparently the development of combined thermal protection [3, 4].

In the present paper, we solve the problem of heating of the shell of a spherically blunted cone in a supersonic airflow at various angles of attack with a laminar boundary-layer flow. In this case, to decrease the maximum surface temperature, we used highly heat-conducting materials for the shell of the streamline apparatus and gas injection from the surface of the porous spherical bluntness.

1. Formulation of the Problem. For the perfect gas model, the system of equations of a spatial boundary layer in a natural coordinate system attached to the outer surface has the form

$$\frac{\partial}{\partial s}(\rho u r_w) + \frac{\partial}{\partial n}(\rho v r_w) + \frac{\partial}{\partial \eta}(\rho w) = 0,$$

$$\rho\Big(u\,\frac{\partial u}{\partial s} + v\,\frac{\partial u}{\partial n} + \frac{w}{r_w}\,\frac{\partial u}{\partial \eta} - \frac{w^2}{r_w}\,\frac{\partial r_w}{\partial s}\Big) = -\frac{\partial p_e}{\partial s} + \frac{\partial u}{\partial n}\Big(\mu\,\frac{\partial u}{\partial n}\Big),$$

$$\rho\Big(u\,\frac{\partial w}{\partial s} + v\,\frac{\partial w}{\partial n} + \frac{w}{r_w}\,\frac{\partial w}{\partial \eta} + \frac{uw}{r_w}\,\frac{\partial r_w}{\partial s}\Big) = -\frac{1}{r_w}\,\frac{\partial p_e}{\partial \eta} + \frac{\partial}{\partial n}\Big(\mu\,\frac{\partial w}{\partial n}\Big), \tag{1}$$

$$\rho c_p\Big(u\,\frac{\partial T}{\partial s} + v\,\frac{\partial T}{\partial n} + \frac{w}{r_w}\,\frac{\partial T}{\partial \eta}\Big) = \frac{\partial}{\partial n}\Big(\mu\,\frac{\partial T}{\partial n}\Big) + u\,\frac{\partial p_e}{\partial s} + \frac{w}{r_w}\,\frac{\partial p_e}{\partial \eta} + \mu\Big[\Big(\frac{\partial u}{\partial n}\Big)^2 + \Big(\frac{\partial w}{\partial n}\Big)^2\Big],$$

$$p = \rho RT/m, \qquad p = p_e(s, \eta).$$

For the porous spherical shell ($0 < s < s_1$) with one-dimensional filtration of the gas injected normally to the surface in the examined coordinate system attached to the body symmetry axis, we have [4]

Tomsk State University, Tomsk 634050. Translated from Prikladnaya Mekhanika i Tekhnicheskaya Fizika, Vol. 43, No. 1, pp. 137–143, January–February, 2002. Original article submitted February 14, 2001; revision submitted April 23, 2001.

0021-8944/02/4301-0114 $27.00

$$(\rho c_p)_1(1-\varphi)\frac{\partial T_1}{\partial t} = \frac{1}{r_1 H_1}\Big[\frac{\partial}{\partial n_1}\Big(r_1 H_1 \lambda_1 (1-\varphi)\frac{\partial T_1}{\partial n_1}\Big) + \frac{\partial}{\partial s}\Big(\frac{r_1\lambda_1}{H_1}(1-\varphi)\frac{\partial T_1}{\partial s}\Big)$$

$$+ \frac{\partial}{\partial \eta}\Big(\frac{H_1\lambda_1}{r_1}(1-\varphi)\frac{\partial T_1}{\partial \eta}\Big)\Big] + (\rho v)_w \frac{r_{1w}}{r_1 H_1}\, c_{p,\mathrm{g}}\,\frac{\partial T_1}{\partial n_1}, \qquad (2)$$

$$0 < n_1 < L, \quad 0 < \eta < \pi, \quad H_1 = (R_N - n_1)/R_N, \quad r_1 = (R_N - n_1)\sin\bar{s}, \quad \bar{s} = s/R_N.$$

For the conical part of the body ($s_1 < s < s_k$), the heat-conduction equation is

$$r_2\rho_2 c_{p2}\frac{\partial T_2}{\partial t} = \frac{\partial}{\partial n_1}\Big(r_2\lambda_2\frac{\partial T_2}{\partial n_1}\Big) + \frac{\partial}{\partial s}\Big(r_2\lambda_2\frac{\partial T_2}{\partial s}\Big) + \frac{1}{r_2}\frac{\partial}{\partial \eta}\Big(\lambda_2\frac{\partial T_2}{\partial \eta}\Big),$$

$$r_2 = (R_N - n_1)\cos\theta + (s - s_1)\sin\theta. \qquad (3)$$

The boundary and initial conditions are written as follows. On the outer surface of the boundary layer ($n \to \infty$), we have

$$u \to u_e(s,\eta), \qquad w \to w_e(s,\eta), \qquad T \to T_e(s,\eta), \qquad (4)$$

where u_e, w_e, T_e, and P_e are determined from the solution of the Euler equations by the method of [5].

On the surface of the streamline body, we have

$$u(s,\eta) = w(s,\eta) = 0, \qquad (\rho v) = (\rho v)_w(s,\eta) = \mathrm{const} \qquad (0 < s < s_1),$$

$$(\rho v) = 0 \qquad (s_1 \leqslant s \leqslant s_k). \qquad (5)$$

On the outer surface of the shell ($0 \leqslant \eta \leqslant \pi$),

$$\Big(\lambda\frac{\partial T}{\partial n}\Big)\Big|_w - \varepsilon_1\sigma T_{1w}^4 = -\lambda_1(1-\varphi)\Big(\frac{\partial T_1}{\partial n_1}\Big)\Big|_w, \qquad \Big(\lambda\frac{\partial T}{\partial n}\Big)\Big|_w - \varepsilon_2\sigma T_{2w}^4 = -\lambda_2\Big(\frac{\partial T_2}{\partial n_1}\Big)\Big|_w. \qquad (6)$$

On the inner surface of the hemisphere and the conical part, the following relations hold [4]:

$$\lambda_1(1-\varphi)\frac{\partial T_1}{\partial n_1}\Big|_{n_1=L} = -\frac{r_{1w}c_{p,\mathrm{g}}(\rho v)_w}{(r_1 H_1)_{n_1=L}}(T_{1L} - T_{\mathrm{in}}), \qquad 0 < s < s_1,$$

$$\lambda_1\frac{\partial T_2}{\partial n_1}\Big|_{n_1=L} = 0, \qquad s_1 \leqslant s \leqslant s_k. \qquad (7)$$

On the conjugation ring "sphere–cone" ($s = s_1$), ideal contact conditions are used, and at $s = s_k$, the adiabatic condition is used:

$$\frac{\lambda_1(1-\varphi)}{H_1}\frac{\partial T_1}{\partial s}\Big|_{s=s_1-0} = \lambda_2\frac{\partial T_2}{\partial s}\Big|_{s=s_1+0}, \quad T_1\Big|_{s=s_1-0} = T_2\Big|_{s=s_1+0}, \quad \frac{\partial T_2}{\partial s}\Big|_{s=s_k} = 0. \qquad (8)$$

In the presence of a plane of flow symmetry, we have

$$\Big(\frac{\partial T_i}{\partial \eta}\Big)\Big|_{\eta=0} = \Big(\frac{\partial T_i}{\partial \eta}\Big)\Big|_{\eta=\pi} = 0, \qquad i = 1, 2. \qquad (9)$$

The initial conditions are

$$T_1\Big|_{t=0} = T_2\Big|_{t=0} = T\Big|_{t=0} = T_{\mathrm{in}}. \qquad (10)$$

In Eqs. (1)–(10), u, v, and w are the mass-average velocity components in the natural coordinates (s, n, η), p, ρ, and T are the pressure, density, and temperature, respectively, t is time, $(\rho v)_w$ is the flow rate of the coolant gas, c_p, λ, and μ are the heat capacity, thermal conductivity, and toughness, respectively, m is the molecular weight, R is the universal gas constant, r_w, r_1, and H_1 are the Lamé factors, φ is the porosity, R_N is the radius of the spherical bluntness, σ is the Stefan–Boltzmann constant, ε_i ($i = 1, 2$) are the emissivities of the shell surface, the normal to the surface n_1 is directed into the depth of the shell, L is the thickness of the shell, and θ is the cone angle; the subscripts e and w correspond to the quantities on the outer surface of the boundary layer and on the surface of the streamline body, respectively, the subscripts 1 and 2 correspond to the condensed phase of the spherical and conical parts of the body, respectively, and the subscripts g, in, and k refer to the gas phase of the porous spherical shell, the initial conditions, and the peripheral region of the shell, respectively; the bar denotes dimensionless quantities.

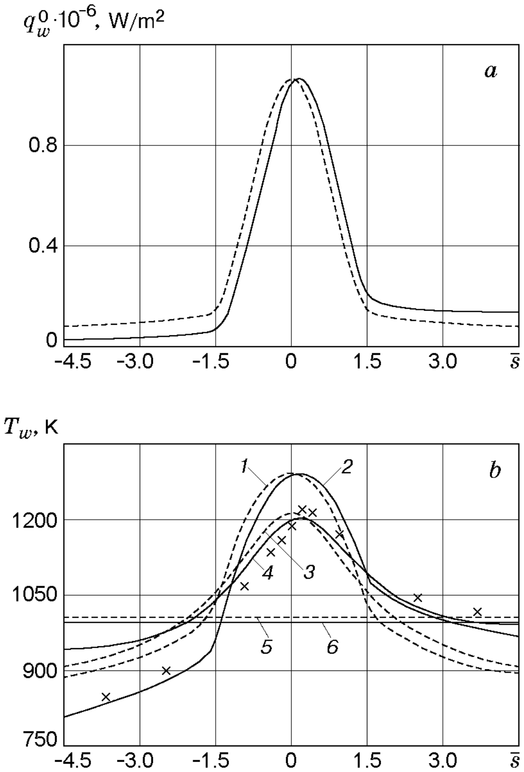

Fig. 1

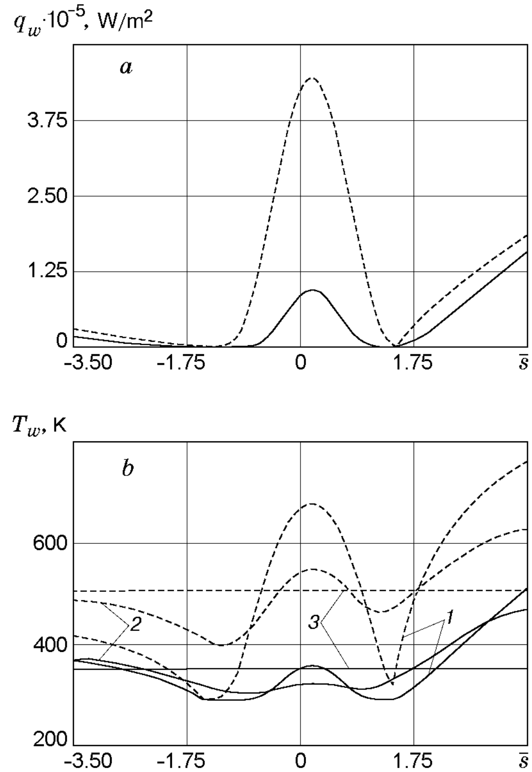

Fig. 2

In (1), the conservation equations are written under the assumption of unchanged composition, which is valid if the composition of the injected gas coincides with the composition of the free-stream flow (air in ours case).

The boundary-value problem (1)–(10) was solved numerically by an iterative-interpolation method [6].

Equations (1) were solved in the Dorodnitsyn–Lees variables for a laminar boundary-layer flow. The three-dimensional unsteady equations (2) and (3) were solved using a locally one-dimensional splitting scheme [7]. The geometry of the model, the pressure at the stagnation point, and the flow rate and law of consumption of the gas injected from the bluntness surface are taken from [8]: the free-stream Mach number $M_\infty = 5$, $R_N = 0.0508$ m, the stagnation pressure $p_{e0} = 3.125 \cdot 10^5$ N/m^2, $(\rho v)_w(\bar{s}, \eta) = \text{const}$, $T_{\text{in}} = 288$ K, $T_{e0} = 1500$ K, the stagnation enthalpy $h_{e0} = 1.536 \cdot 10^6$ J/kg, $\varepsilon_1 = \varepsilon_2 = 0.85$, $L = 2.2 \cdot 10^{-3}$ m, $\theta = 5°$, the angle of attack $\beta = 10°$, and $\varphi = 0.34$.

As the material of the shell, we considered asbestos cement [$\lambda_i = 0.349$ W/(m $\cdot$ K), $c_{pi} = 837$ J/(kg $\cdot$ K), $\rho_i = 1800$ kg/m^3, $i = 1$, 2] and copper [$\lambda_i = 386$ W/(m $\cdot$ K), $c_{pi} = 370$ J/(kg $\cdot$ K), $\rho_i = 8950$ kg/m^3, $i = 1$, 2] [9].

2. Analysis of the Numerical Solution. Figure 1 gives the convective heat flux from the gas phase q_w^0 and the surface temperature T_w versus the coordinate $\bar{s}$ on the windward and leeward sides of the symmetry plane at $(\rho v)_w = 0$. The solid curves correspond to an angle of attack $\beta = 10°$, and the dashed curve correspond to $\beta = 0$. Figure 1a corresponds to the time $t = 0$. In Fig. 1b, curves 1 and 2 are obtained for a shell made of asbestos cement, curves 3 and 4 correspond to a copper shell, and curves 5 and 6 correspond to the condition $\lambda_i \to \infty$ ($i = 1$ and 2). The temperature distributions over the shell surface are calculated for steady-state ($t \to \infty$) heating of the body, and the calculations of the heating of a copper shell ignoring heat flow along the circumferential coordinate η are shown by crosses.

From Fig. 1 it follows that the region of maximum temperature of the impermeable shell surface coincides with the region of maximum thermal flux for a laminar boundary-layer in the vicinity of the stagnation point. In this case, a change of the angle of attack causes a shift of the maxima relative to the center of symmetry of the streamline body.

For the non-heat-conducting material of the shell, the surface temperature is equal to the equilibrium radiation temperature T_{wp} because for asbestos cement, the heating process is one-dimensional. The temperature T_{wp} determined from the condition of conservation of energy on the porous and conical surfaces [4]

$$q_w + c_{p,\text{g}}(\rho v)_w(T_{\text{in}} - T_{wp}) = \varepsilon_1 \sigma T_{wp}^4, \qquad q_w = \varepsilon_2 \sigma T_{wp}^4,$$

is maximum attainable surface temperature in the absence of heat flow in the longitudinal and circumferential directions. For the highly heat-conducting material of the shell, the maximum surface temperature decreases appreciably. At the same time, the heat flow along the longitudinal and circumferential coordinates increases the surface temperature of the conical part (especially on the leeward side) compared to T_{wp}. Neglect of heat flow in the circumferential direction for a spatial flow around the body leads to an increase of T_w on the windward side and a decrease of it on the leeward side. As $\lambda_i \to \infty$ ($i = 1, 2$) there is a considerable decrease in the temperature of the spherical part of the body and equalization of the temperature profile in the streamline material, and values of the surface temperature agree with the calculations of [4].

We consider the effect of the coolant gas flow from the surface bluntness. Figure 2 gives distributions of the heat flux q_w at $t = 0$ and the stationary surface temperature T_w for flow at incidence. The solid and dashed curves are obtained for values $(\rho v)_w = 1.626$ and 0.813 kg/(m$^2\cdot$ sec), respectively. Injection of a coolant gas from the porous bluntness decreases considerably the heat flux on the spherical part. In this case, for $(\rho v)_w = 0.813$ kg/(m$^2\cdot$ sec) there is a linear dependence $q_w(\rho v)_w$, which agrees well with the formula of [10] $q_w/q_w^0 = 1 - k(\rho v)_w/(\alpha/c_p)^0$, where $k = 0.57$–0.61. Furthermore, at $(\rho v)_w = 1.626$ kg/(m$^2\cdot$ sec), the dependence of the ratio of the heat flux at the critical point to the corresponding value of q_w^0 in the absence of injection q_w/q_w^0 on the injection parameter $(\rho v)_w/(\alpha/c_p)^0$ is close to that obtained experimentally by Feldhuhn [8], who studied the effect of intense injections on heat flows to a porous spherical surface.

As follows from Fig. 2b, for injection of a coolant gas, the dependence $T_w(\bar{s})$ differs qualitatively from the distribution of $T_w(\bar{s}, \eta)$ at $(\rho v)_w = 0$ for various values of λ_i. In Fig. 2b, curves 1 correspond to the shell from asbestos cement with values of T_w coincident with the value of the radiation temperature of the surface T_{wp}, curves 2 are obtained for the copper shell, and curves 3 correspond to the limiting case $\lambda_i \to \infty$. For $(\rho v)_w = 0.813$ kg/(m$^2\cdot$ sec) with increase in λ_i, the values of T_w on the windward side of the conical part of the body decrease in comparison with T_{wp} because of heat sink into the porous bluntness, and on the leeward side, heat flow results in the surface temperature becoming much higher than the equilibrium radiation temperature. With increase in the flow rate of the coolant gas, the nature of the dependences $T_w(\bar{s})$ and $T_{wp}(\bar{s})$ on the conical part of the body does not change. On the porous part of the shell, an increase in the injection parameter and thermal conductivity of the material leads to intense heat sink from the conical surface and a decrease and subsequent equalization of the temperature of the spherical bluntness.

In the case of $\lambda_i \to \infty$ (curve 3 in Fig. 2b) for $(\rho v)_w \neq 0$, the surface temperature is less than half that in the case $(\rho v)_w = 0$ (see Fig. 1). This result confirms that it is reasonable to use highly heat-conducting materials to ensure intense heat sink to the region of the permeable bluntness.

It is of interest to study the distribution of $T_w(\bar{s}, \eta)$ in the steady-state regime for various flow rates of the coolant gas and materials with various thermal properties. Figure 3 shows distributions of the heat flux and surface temperature along the longitudinal coordinate for the copper shell. As in Figs. 1 and 2, the values of q_w correspond to the time $t = 0$, and T_w corresponds to steady-state heating of the body. The dot-and-dashed, dashed, and solid curves correspond to 0, $(\rho v)_w = 1.626$, and 0.813 kg/(m$^2\cdot$ sec), respectively, and curves 1, 2, and 3 correspond to the surface temperature at $\eta = 0$, $\pi/2$, and π, respectively. Figure 4 shows the steady-state temperature field for the material with low heat-conductivity (asbestos cement) (the notation is the same as in Fig. 3).

As one might expect, the maximum surface temperature is reached on the windward side of the shell and corresponds to the maximum convective heat flux from the gas phase for $\eta = 0$ both with and without injection of a coolant gas. An analysis of Figs. 3 and 4 shows that with constant injection of the coolant gas along the generatrix, the value of T_{wp} at the stagnation point on the spherical part of the body exceeds the corresponding value T_w for the copper shell. At the same time, in the vicinity of the "sphere–cone" conjugation ($\bar{s} = \bar{s}_1$), heat flow results in the temperature T_w becoming much higher than the surface temperature of the non-heat-conducting shell.

The crosses in Figs. 3 and 4 correspond to calculations in a simplified formulation for the convective heat-transfer coefficient taken from [11] and for $\eta = \pi/2$ and $(\rho v)_w = 0$. It should be noted that in the absence of injection of a coolant gas, the results of solution of the problem in the separate and conjugate formulations agree fairly well.

Besides the solution of the problem in the conjugate formulation, we studied the question of whether the use the separate formulation is reasonable in the case of specified convective heat-transfer coefficient for the isothermal (at the initial time) surface of the body. Figure 5 shows the dependence $T_w(\bar{s})$ in the flow symmetry plane for

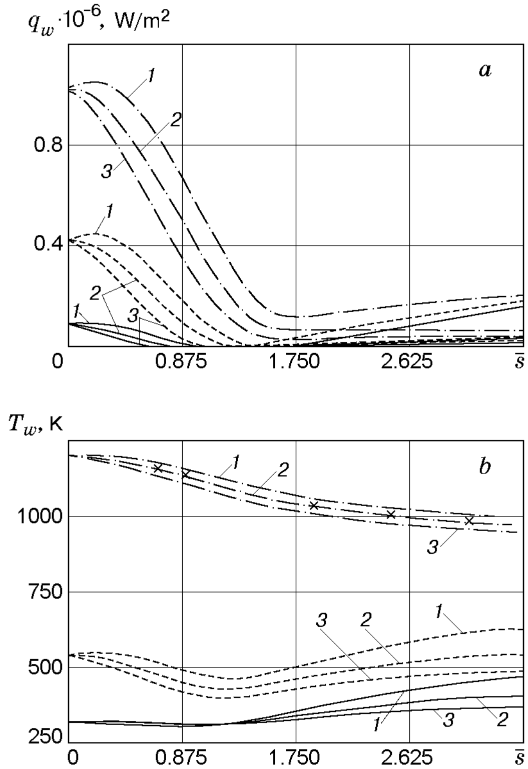

Fig. 3

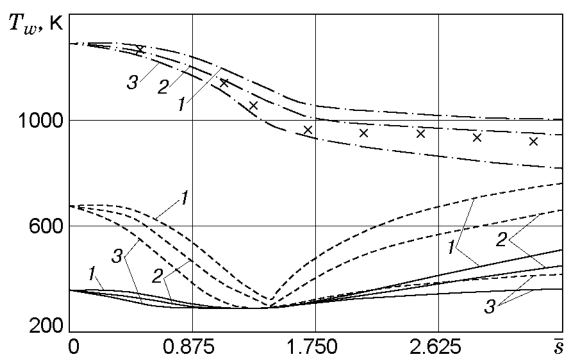

Fig. 4

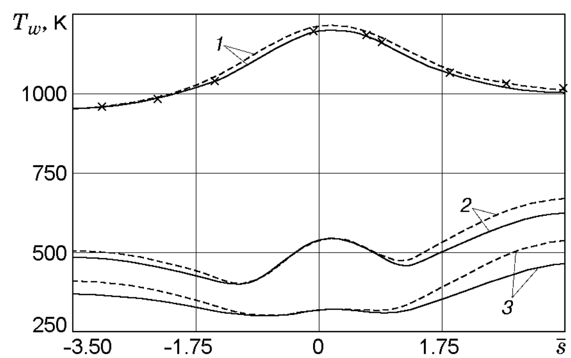

Fig. 5

steady-state flow around a copper shell ($\beta = 10°$). The solid curves correspond to the solution in the conjugate formulation, and the dashed curves correspond to the separate formulation. Curves 1–3 were obtained for $(\rho v)_w = 0$, 0.813, and 1.626 kg/(m$^2 \cdot$ sec), respectively, and the crosses are results of calculation in the separate formulation for the heat-transfer coefficient taken from [11], in the flow symmetry plane for $(\rho v)_w = 0$. From Fig. 5 it follows that the separate formulation can be used to calculate the temperature field of the shell without injection from the surface using the value of the heat-transfer coefficient for an isothermal (at the initial time) surface or the value determined from the formulas of [11]. In the case of injection in the screen zone, the approximate approach using the coefficient of heat transfer to an isothermal surface results in a considerable increase in surface temperature compared to the exact solution of the heating problem in the conjugate formulation. This is due to the complex character of heat transfer in the case of a nonisothermal surface. Under these conditions, as is shown in [1], the expression for the heat-transfer coefficient includes the term $(\partial T_w/\partial \bar{s})/(T_{e0} - T_w)$, whose effect becomes significant in the thermal screen zone, where considerable temperature gradients $\partial T_w/\partial \bar{s}$ occur.

This work was supported by the Russian Foundation for Fundamental Research (Grant No. 99-01-00352).

REFERENCES

1. V. I. Zinchenko, *Mathematical Modeling of Conjugate Heat- and Mass-Transfer Problems* [in Russian], Izd. Tomsk Univ., Tomsk (1985).
2. V. A. Bashkin and S. M. Reshet'ko, "Maximum temperature of a bluntness taking into account thermal conductivity," *Uch. Zap. TSAGI*, **20**, No. 5, 53–59 (1989).
3. V. I. Zinchenko, A. G. Kataev, and A. S. Yakimov, "Temperature regimes of streamline bodies with gas injection from the surface," *Prikl. Mekh. Tekh. Fiz.*, No. 6, 57–64 (1992).
4. V. I. Zinchenko and A. S. Yakimov, "Heat-transfer characteristics in flow around a spherically blunted cone at incidence and gas injection from a blunted surface," *Prikl. Mekh. Tekh. Fiz.*, **40**, No. 4, 162–169 (1999).
5. V. A. Antonov, V. D. Go'ldin, and F. M. Pakhomov, *Aerodynamics of Bodies with Injection* [in Russian], Tomsk State Univ., Tomsk (1990).
6. A. M. Grishin, V. N. Bertsun, and V. I. Zinchenko, Iteratvie–Interpolation Method and Its Applications [in Russian] Tomsk State Univ., Tomsk (1981).
7. A. A. Samarskii, *Introduction to the Theory of Difference Schemes* [in Russian], Nauka, Moscow (1971).
8. R. H. Feldhuhn, "Heat transfer from a turbulent boundary layer on a porous hemisphere," AIAA Paper No. 119, New York (1976).
9. Yu. V. Polezhaev and F. B. Yurevich, *Thermal Protection* [in Russian], Énergiya, Moscow (1976).
10. N. A. Anfimov and V. V. Al'tov, "Heat transfer, friction, and mass transfer in a laminar multicomponent boundary layer with injection of foreign gases," *Teplofiz. Vys. Temp.*, No. 3, 409–420 (1965).
11. B. A. Zemlyanskii and G. I. Stepanov, "Calculation of heat exchange for spatial hypersonic air flows around thin blunted cones," *Izv. Akad. Nauk SSSR, Ser. Mekh. Zhidk. Gaza*, No. 5, 173–177 (1981).